DE GRUYTER Open Mathematics 2025; 23: 20240121

Research Article

Hleil Alrweili*

Statistical inference and data analysis of the record-based transmuted Burr X model

https://doi.org/10.1515/math-2024-0121
received March 23, 2024; accepted December 20, 2024

Abstract: Probability distribution has proven its usefulness in almost every discipline of human endeavors. A novel extension of Bur X distribution is developed in this study employing the record-based transmuted mapping technique, which can be used to fit skewed and complex data. We referred to this novel distribution as a record-based transmuted Burr X model. We established the shape of the probability density function and hazard function. Numerous statistical and mathematical properties are provided, including quantile function, moment, and ordered statistics of the proposed model. Further, we obtain the estimation of the model parameters using the maximum likelihood estimation method, and four sets of Monte Carlo simulation studies are carried out to evaluate the efficiency of these estimates. Finally, the practical applicability of the developed model is demonstrated by analyzing three data sets, comparing its performance with several well-known distributions. The results highlight the flexibility and accuracy of the model, establishing it as a powerful and reliable tool for advanced statistical modeling in environmental and survival research.

Keywords: Burr X model, hazard function, ordered statistics, probability models, transmuted mapping

MSC 2020: 60E05, 62E17, 62H12, 62G30, 62F10

1 Introduction

The utilization of asymmetrical statistical distributions is widespread across nearly all disciplines, reflecting their fundamental role in understanding and interpreting uncertainty in various contexts, notably engineering, industrial, medical sciences, insurance, and environmental. As a result, it appears essential to obtain statistical models, which are a critical and challenging task. However, sometimes, there are cases in which these statistical distributions are not suitable for analyzing several data sets. For this, the author has worked to apply numerous methods for obtaining novel families of distributions that extend well-known models. These novel-generated family models have a crucial role in fitting skewed data sets. In relation to this, we refer several previous studies that have investigated the established probability distributions, specifically those conducted by Hamedani et al. [1], Cordeiro and Brito [2], Marshall and Olkin [3], Mahdavi and Kundu [4], Hassan et al. [5], Moakofi et al. [6], Eghwerido et al. [7], Sapkota et al. [8], Meraou and Raqab [9], Meraou et al. [10], and Thomas and Chacko [11].

In this context, Balakrishnan and He [12] proposed one of these procedures called the record-based transmuted mapping technique that is considered in numerous applied fields, such as insurance, medical science, biology, environment, and finance. Its cumulative distribution function (cdf) and corresponding probability distribution function (pdf) can be formulated as

$$G(x,\varphi) = F(x,\varphi) + \theta[1 - F(x,\varphi)]\log[1 - F(x,\varphi)], \quad x \in \mathbb{R}, \; \theta \in [0,1] \tag{1}$$

*** Corresponding author: Hleil Alrweili,** Department of Mathematics, College of Science, Northern Border University, Arar, Saudi Arabia, e-mail: Hleil.Alrweili@nbu.edu.sa

and

$$g(x,\varphi) = f(x,\varphi)[1 - \theta - \theta \log(1 - F(x,\varphi))], \quad (2)$$

where $F(x;\varphi)$ and $f(x;\varphi)$ represent the cdf and pdf of the parent distribution with parameter φ.

In the last few decades, the record-based transmuted mapping technique has been developed by different researchers in the literature. For example, Tanis and Saracoglu [13] introduced a record-based Weibull model by taking the Weibull distribution as the baseline model and establishing different properties of the proposed model. Arshad et al. [14] introduced a novel approach of generalization exponential distribution using record transmuted mapping procedure, and they studied different mathematical and distributional properties of the proposed model. Notably, the record-based transmuted model of Tanis proposes record-based transmuted Lindley distribution [15], and he applied the suggested model to COVID-19 patient data to demonstrate the potential of the proposed model among other new distributions. Many authors discussed digital transformation and employees with 4 years after COVID-19. In the same way, Sakthivel and Nandhini [16] provided the record transmuted power Lomax model with applications to the reliability area. Sobhi and Mashail [17] discussed moments of dual generalized order statistics and characterization for transmuted exponential model. Abu El Azm et al. discussed new transmuted generalized Lomax distribution. Mohamed et al. [18] introduced transmuted Topp-Leone length biased exponential model under competing risk model. A record-based transmuted Nadarajah-Haghighi model is defined by Kumar et al. [19].

As far as we know, the Burr X distribution (BXD) is a versatile statistical tool for modeling complex and asymmetric data and complementary risk scenarios. It has numerous applications in many practical cases, like fitting the lifetime record in the engineering field. One may refer to the studies of Usman and Ilyas [20], Al-Babtain et al. [21], Fayomi et al. [22], Raqab and Kundu [23], Yıldırım et al. [24], Korkmaz et al. [25], and Merovci et al. [26].

Surles and Padgett [27] provided the Burr X (BX) model. The associated probability density and cumulative density functions of the BX model are expressed respectively as follows:

$$f(x;\,\alpha,\beta) = 2\alpha^2\beta x^{2\beta-1}e^{-(\alpha y^{\beta})^2}, \quad x > 0 \quad (3)$$

and

$$F(x;\,\alpha,\beta) = 1 - e^{-(\alpha y^{\beta})^2}. \quad (4)$$

In the present study, we take the BXD and apply the record-transmuted mapping technique to construct a new family of distributions that can be enhanced fitting capabilities in various practical applications when assessed against existing models. We referred to it as the record-transmuted Bur X (RT-BX) model; we sometimes called it record-transmuted power Bur X (RT-PBX) model. The proposed model can take a variety of shapes. As well as, we can obtain the basic distribution as a special case. The hazard function of the proposed distribution can exhibit various shapes, including increasing and decreasing. Further, various distributional and mathematical properties of the RT-BX model, like MGF, ordered statistics, and quantile function, are obtained as well and five entropy estimators for the RT-BX model are computed.

The rest of this study is outlined as follows: In Section 2, we construct the RT-BX model and thoroughly discuss its behavior of pdf and hazard rate function. Numerous mathematical and statistical properties are established in Section 3. In Section 4, several suggested entropy measures for the recommended distribution are defined, and its estimation parameters are developed in Section 5 by employing the maximum likelihood estimation (MLE) procedure. In Section 6, simulation experiment studies are explored to see the applicability of the MLE technique. Finally, three real-life applications are analyzed in Section 7 for validation purposes. Some important remarks are presented in Section 8.

2 Record-based transmuted BXD

2.1 Model description

In this subsection, we proposed certain distribution properties of the RT-BX model, such as probability density, cumulative density functions, survival, and hazard rate functions.

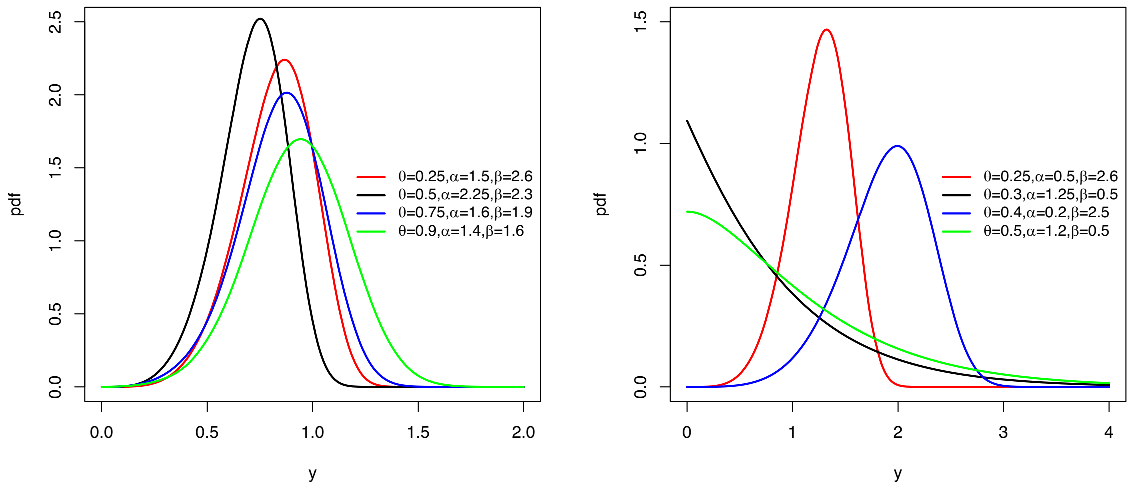

Figure 1: Graphs of the RT-BX density for numerous parameter values.

Let the BXD with parameters α and β be parent distribution. According to equations (1)–(4), the corresponding cumulative density function and probability density function of the proposed RT-BX model are, respectively, expressed as

$$H_y(y) = 1 - e^{-(\alpha y^{\beta})^2}[1 + \theta(\alpha y^{\beta})^2] \tag{5}$$

and

$$h_Y(y) = 2\alpha^2 y^{2\beta-1} e^{-(\alpha y^{\beta})^2}[1 - \theta + \theta(\alpha y^{\beta})^2]. \tag{6}$$

Figure 1 shows curves of the probability density function of the RT-BX model for different parameter values. From these plots, obviously the density is positively skewed and symmetric and decreasing when $0 < \beta \le 1/2$ and uni-modal if $\beta \ge 1/2$. Theorem 1 ensures this conclusion.

Next the survival function with the associated hazard rate function of the RT-BX model can be formulated, respectively, by

$$S_Y(y) = e^{-(\alpha y^{\beta})^2}[1 + \theta(\alpha y^{\beta})^2]$$

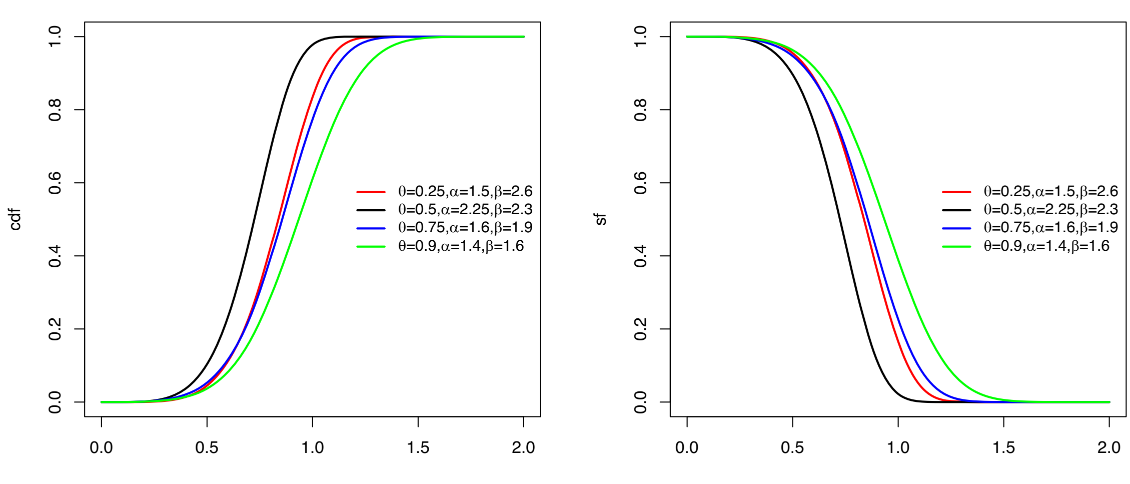

Figure 2: Cumulative and survival plots for the RT-BX model using different values of the parameters.

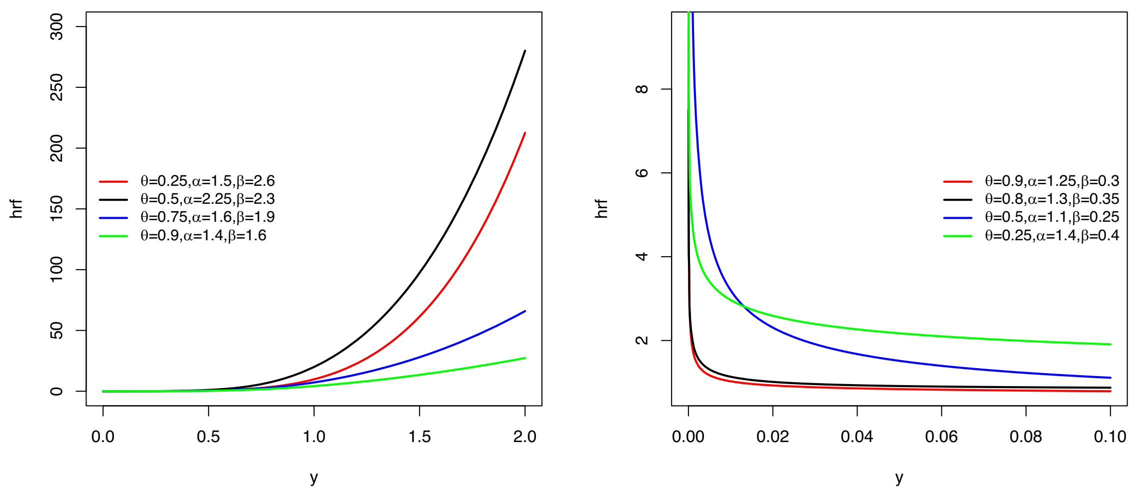

Figure 3: Hazard rate function plots for the RT-BX model using different values of the parameters.

and

$$hr_Y(y) = \frac{2\alpha^2 y^{2\beta-1}[1-\theta+\theta(\alpha y^\beta)^2]}{1+\theta(\alpha y^\beta)^2}. \tag{7}$$

The cumulative, survival, and hazard rate function plots of the RT-BX model are sketched in Figures 2 and 3, respectively. From Figure 3, it can be observed that the hazard rate function increases if $\beta \geq 1/2$ and decreases if $0 < \beta \leq 1/2$, which shows the flexibility of the proposed RT-BX model, and Theorem 2 confirms this conclusion.

Next the cumulative hazard rate function of the RT-BX is

$$CH_Y(y) = (\alpha y^\beta)^2 - \ln[1+\theta(\alpha y^\beta)^2].$$

The reversed hazard rate function can be formulated as

$$R_Y(y) = \frac{2\alpha^2 y^{2\beta-1} e^{-(\alpha y^\beta)^2}[1-\theta+\theta(\alpha y^\beta)^2]}{1-e^{-(\alpha y^\beta)^2}[1+\theta(\alpha y^\beta)^2]}.$$

2.2 Behavior of density and hazard rate functions of the RT-BX model

Theorem 1. *When $\beta > \frac{1}{2}$, the density of the RT-BX model is unimodal, and it is decreasing if $0 < \beta \leq \frac{1}{2}$.*

Proof. Put $t = (\alpha y^\beta)^2$, then $y = \left[\frac{t^{1/2}}{\alpha}\right]^{1/\beta}$. So, the density function of the RT-BX model is rewritten as a function of t, and it is given as

$$\Phi(t) = h\left(\left[\frac{t^{1/2}}{\alpha}\right]^{1/\beta}\right) = 2\alpha^{\frac{1}{\beta}} t^{1-\frac{1}{2\beta}} e^{-t}(1-\theta+\theta t). \tag{8}$$

Based on equation (8), the first derivative of $\ln\Phi(t)\left(\frac{\partial \ln\Phi(t)}{\partial t}\right)$ can be written as

$$\frac{\partial \ln\Phi(t)}{\partial t} = \frac{2\beta-1}{2\beta t} + \frac{\theta}{1-\theta+\theta t} - 1. \tag{9}$$

Clearly, equation (9) is a decreasing function of t if $\beta > \frac{1}{2}$ and we have

$$\lim_{t\mapsto 0} \frac{\partial \ln\Phi(t)}{\partial t} = +\infty, \quad \lim_{t\mapsto\infty} \frac{\partial \ln\Phi(t)}{\partial t} = -1,$$

which confirms that the function $\frac{\partial \ln\Phi(t)}{\partial t}$ change single positive to negative. Consequently, the density of the RT-BX distribution is unimodal.

By using the same steps, if $0 < \beta \le \frac{1}{2}$, then it can be easily observed that the function $\frac{\partial \ln \Phi(t)}{\partial t}$ is increasing and

$$\lim_{t \mapsto 0} \frac{\partial \ln \Phi(t)}{\partial t} = -\infty \lim_{t \mapsto \infty} \frac{\partial \ln \Phi(t)}{\partial t} = -1.$$

This ensures that the function $\frac{\partial \ln \Phi(t)}{\partial t}$ is negative and the density of the RT-BX model is decreasing. □

Theorem 2. *For $\beta > \frac{1}{2}$, the hazard rate for the RT-BX distribution have increasing and it is decreasing functions if $0 < \beta \le \frac{1}{2}$.*

Proof. Let

$$U(t) = \frac{\partial^2 \ln \Phi(t)}{\partial t^2} = -\frac{2\beta(2\beta - 1)}{(2\beta t)^2} - \frac{\theta^2}{(1 - \theta + \theta t)^2} + \frac{\theta^2}{(1 + \theta t)^2}.$$

Hence, from the above equation the function $U(t)$ is positive if $\beta > \frac{1}{2}$, and it is negative for $0 < \beta \le \frac{1}{2}$. As a result, by applying the theorem of Glaser [28], the hazard rate function of the RT-BX model is increasing if $\beta > \frac{1}{2}$ and decreasing if $0 < \beta \le \frac{1}{2}$. □

3 Mathematical properties

We developed here various statistical characteristics of the recommended RT-PBX distribution. From now on, let $Y \sim \text{RT-BX}(\theta, \alpha, \beta)$.

3.1 Quantile function of the RT-BX model

The quantile function y_u of Y is obtained from equation (5), and it is defined by

$$y_u = \left\{\alpha^{-1}\left[-\frac{1}{\theta} - W_{-1}\left(\frac{u-1}{\theta e^{\frac{1}{\theta}}}\right)\right]^{1/2}\right\}^{1/\beta}, \quad 0 < u < 1. \tag{10}$$

Proof. By setting equation (5) equal to u, we obain

$$\begin{aligned}
1 - e^{-(\alpha y^\beta)^2}[1 + \theta(\alpha y^\beta)^2] &= u \\
e^{-(\alpha y^\beta)^2}[1 + \theta(\alpha y^\beta)^2] &= 1 - u \\
e^{-(\alpha y^\beta)^2}\left[\frac{1}{\theta} + (\alpha y^\beta)^2\right] &= \frac{1-u}{\theta} \\
e^{-(\alpha y^\beta)^2}\left[-\frac{1}{\theta} - (\alpha y^\beta)^2\right] &= \frac{u-1}{\theta} \\
e^{-(\alpha y^\beta)^2 - \frac{1}{\theta}}\left[-\frac{1}{\theta} - (\alpha y^\beta)^2\right] &= \frac{u-1}{\theta e^{\frac{1}{\theta}}}.
\end{aligned}$$

Evidently $(u-1)/\theta e^{1/\theta} \in [-1/e, 0)$ and $-(\alpha y^\beta)^2 - \frac{1}{\theta} \in (-\infty, -1]$. Hence, after applying the negative branch of the Lambert W function, we obtain

$$-(\alpha y^\beta)^2 - \frac{1}{\theta} = W_{-1}\left(\frac{u-1}{\theta e^{\frac{1}{\theta}}}\right)$$

$$(\alpha y^{\beta})^2 = -\frac{1}{\theta} - W_{-1}\left(\frac{u-1}{\theta e^{\frac{1}{\theta}}}\right)$$

$$y = \left\{\alpha^{-1}\left[-\frac{1}{\theta} - W_{-1}\left(\frac{u-1}{\theta e^{\frac{1}{\theta}}}\right)\right]^{1/2}\right\}^{1/\beta},$$

which completes the proof. By replacing u by $\frac{1}{4}$, $\frac{1}{2}$, and $\frac{3}{4}$ in (10), the first and third quantiles are obtained, respectively.

The skewness ($\mathcal{S}$) and kurtosis ($\mathcal{K}$) measures of the recommended RT-BX model are provided to be

$$\mathcal{S} = \frac{u_{1/4} + u_{3/4} - 2u_{1/2}}{y_{3/4} - u_{1/4}}$$

and

$$\mathcal{K} = \frac{y_{7/8} - u_{5/8} + y_{3/8} - y_{1/8}}{y_{6/8} - y_{2/8}}.$$ □

3.2 Moments with related measures

The kth moment of Y is

$$\mu_k' = \frac{1}{\beta}\alpha^{2+\beta(k+2\beta)}\left\{\Gamma\left(\frac{1}{2\beta}, 0\right)(1-\theta) + \theta\Gamma\left(\frac{1}{2\beta} + 1, 0\right)\right\}, \tag{11}$$

where, $\Gamma(a, b)$ denotes incomplete gamma function, and it is expressed as $\Gamma(a, b) = \int_b^{\infty} w^{a-1}e^{-w}\mathrm{d}w$.

Proof.

$$\begin{aligned}\mu_k' &= \int_0^{\infty} y^k h_Y(y)\mathrm{d}y \\ &= 2\alpha^2\int_0^{\infty} y^{k+2\beta-1}e^{-(\alpha y^{\beta})^2}(1-\theta+\theta(\alpha y^{\beta})^2)\mathrm{d}y.\end{aligned} \tag{12}$$

Let $t = (\alpha y^{\beta})^2$, which implies that $y = \left(\frac{t^{1/2}}{\alpha}\right)^{1/\beta}$. Then, equation (12) can be rewritten as

$$\begin{aligned}\mu_k' &= \frac{\alpha^{\beta(k+2\beta)+2}}{\beta}\int_0^{\infty} e^{-t}t^{\frac{1-2\beta}{\beta}}(1-\theta+\theta t)\mathrm{d}t \\ &= \frac{\alpha^{\beta(k+2\beta)+2}}{\beta}\left(\int_0^{\infty} t^{\frac{1}{2\beta}-1}e^{-t}\mathrm{d}t - \theta\int_0^{\infty} t^{\frac{1}{2\beta}-1}e^{-t}\mathrm{d}t + \theta\int_0^{\infty} t^{\frac{1}{2\beta}}e^{-t}\mathrm{d}t\right) \\ &= \frac{1}{\beta}\alpha^{2+\beta(k+2\beta)}\left\{\Gamma\left(\frac{1}{2\beta}, 0\right)(1-\theta) + \theta\Gamma\left(\frac{1}{2\beta} + 1, 0\right)\right\},\end{aligned}$$

which completes the proof. Consequently, from equation (11), the mean and second-ordered moment of Y are expressed, respectively, as

$$\mu_1' = \frac{1}{\beta}\alpha^{2+\beta(1+2\beta)}\left\{\Gamma\left(\frac{1}{2\beta}, 0\right)(1-\theta) + \theta\Gamma\left(\frac{1}{2\beta} + 1, 0\right)\right\}$$

and

$$\mu_2' = \frac{1}{\beta}\alpha^{2+\beta(2+2\beta)}\left\{\Gamma\left(\frac{1}{2\beta}, 0\right)(1-\theta) + \theta\Gamma\left(\frac{1}{2\beta} + 1, 0\right)\right\}.$$ □

The variance and coefficient of variation ($\mathcal{V}$) of Y are

$$\mathrm{Var}(Y) = \mu_2' - \mu_1'^2 \quad \text{and} \quad \mathcal{V} = \frac{\sqrt{\mu_2' - \mu_1'^2}}{\mu_1'}.$$

The moment generating function (MGF) of Y is obtained as

$$\begin{aligned} M_Y(t) = E[e^{ty}] &= \int_0^\infty e^{ty} h_Y(y)\mathrm{d}y \\ &= 2\alpha^2 \int_0^\infty e^{ty} y^{2\beta-1} e^{-(\alpha y^\beta)^2}(1 - \theta + \theta(\alpha y^\beta)^2)\mathrm{d}y \\ &= \frac{1}{\beta} \int_{j=0}^{\infty} \frac{t^j \alpha^{2+\beta j+2\beta}}{j!} \left\{\Gamma\left(\frac{1}{2\beta}, 0\right)(1 - \theta) + \theta\Gamma\left(\frac{1}{2\beta} + 1, 0\right)\right\}. \end{aligned} \tag{13}$$

The proposed statistical property values of the RT-BX model are tabulated in Tables 1 and 2 by applying various choices of θ, α, and β. The same can easily be observed for these quantities from the plots presented in Figure 4. From these results of mathematical properties, we can see that

Table 1: Distinct records of mathematical properties for the RT-BX model at θ = 0.5

	α	μ_1'	Var	$\mathcal{V}$	$\mathcal{S}$	$\mathcal{K}$
β = 0.75	0.5	3.0334	3.4198	0.6096	0.8183	0.6445
	1	1.2038	0.5386	0.6096	0.8183	0.6445
	1.5	0.7011	0.1827	0.6096	0.8183	0.6445
	2	0.4777	0.0848	0.6096	0.8183	0.6445
β = 1.5	0.5	1.6533	0.3001	0.3313	−0.0135	−0.2945
	1	1.0415	0.1191	0.3313	−0.0135	−0.2945
	1.5	0.7948	0.0694	0.3313	−0.0135	−0.2945
	2	0.6561	0.0473	0.3313	−0.0135	−0.2945
β = 2.25	0.5	1.3794	0.1015	0.2310	−0.3483	−0.0323
	1	1.0136	0.0548	0.2310	−0.3483	−0.0323
	1.5	0.8465	0.0382	0.2310	−0.3483	−0.0323
	2	0.7449	0.0296	0.2310	−0.3483	−0.0323

Table 2: Distinct records of mathematical properties for the RT-BX model at θ = 0.75

	α	μ_1'	Var	$\mathcal{V}$	$\mathcal{S}$	$\mathcal{K}$
β = 0.75	0.5	3.4122	3.4976	0.5481	0.7177	0.5191
	1	1.3541	0.5508	0.5481	0.7177	0.5191
	1.5	0.7886	0.1868	0.5481	0.7177	0.5191
	2	0.5374	0.0868	0.5481	0.7177	0.5191
β = 1.5	0.5	1.7713	0.2745	0.2958	−0.0858	−0.1425
	1	1.1159	0.1089	0.2958	−0.0858	−0.1425
	1.5	0.8516	0.0634	0.2958	−0.0858	−0.1425
	2	0.7030	0.0432	0.2958	−0.0858	−0.1425
β = 2.25	0.5	1.4484	0.0886	0.2055	−0.4165	0.2257
	1	1.0643	0.0478	0.2055	−0.4165	0.2257
	1.5	0.8888	0.0334	0.2055	−0.4165	0.2257
	2	0.7822	0.0258	0.2055	−0.4165	0.2257

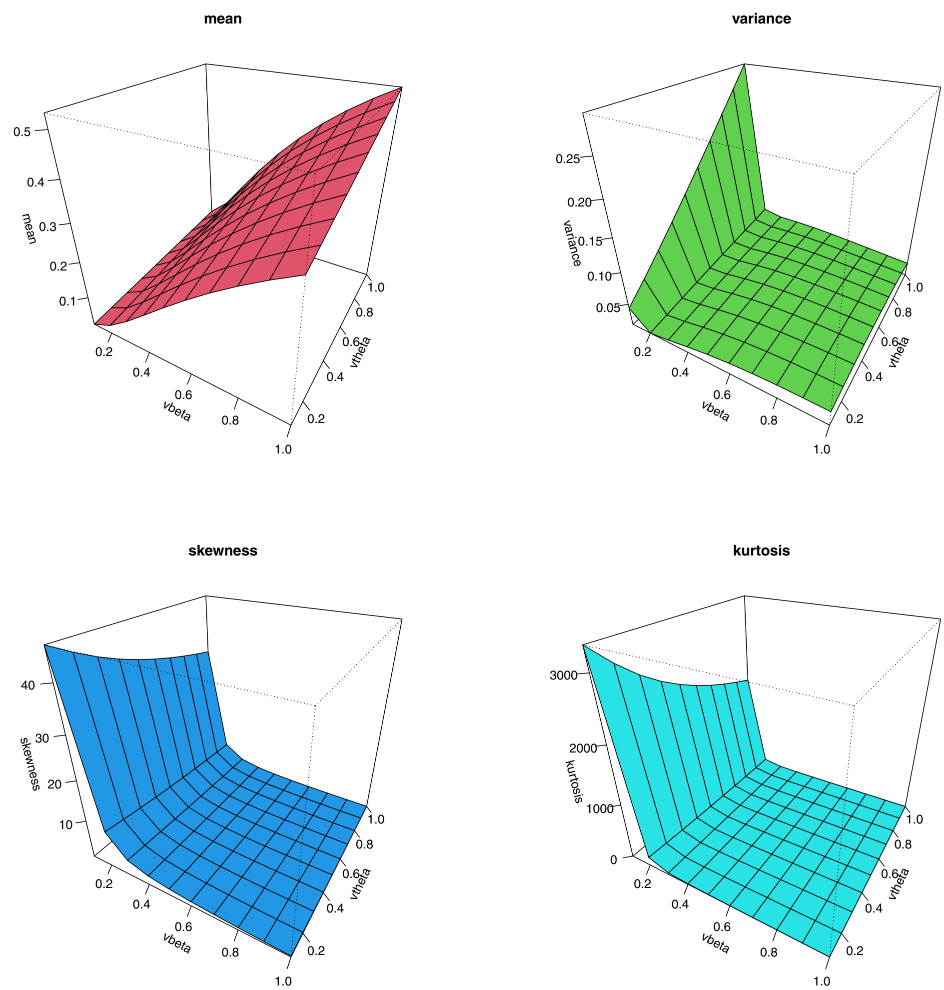

Figure 4: 3D curves of proposed statistical measures considering RT-BX with various selected parameter records.

(1) The findings indicate that μ_1' and Var values decrease with the parameter values, whereas the values of $\mathcal{V}$, $\mathcal{S}$, and $\mathcal{K}$ are fixed.
(2) Now, β increases and α and θ are fixed, the measures of μ_1', Var, $\mathcal{V}$, and $\mathcal{S}$ decrease.
(3) If θ tend to increase when β and θ are fixed, the records of μ_1' and Var tend to increase, but the values of $\mathcal{V}$, $\mathcal{S}$, and $\mathcal{K}$ decrease.

3.3 Order statistics

Let $Y \sim \text{RT-BX}(\theta, \alpha, \beta)$ and $y_{(1)} < \ldots < y_{(n)}$ represent the order statistics of the random sample from Y. Then, the rth density function of Y is written as

$$\begin{aligned} k_{r:n}(y) &= \frac{n!h(y)}{(r-1)!(n-r)!}[H(y)]^{r-1}[1-H(y)]^{n-r} \\ &= \frac{n!g(t)}{(r-1)!(n-r)!}\sum_{m=0}^{n-r}(-1)^m\binom{n-r}{m}[H(y)]^{m+r-1} \\ &= \frac{2n!\alpha^2 y^{2\beta-1}e^{-(\alpha y^{\beta})^2}[1-\theta+\theta(\alpha y^{\beta})^2]}{(r-1)!(n-r)!}\sum_{m=0}^{n-r}(-1)^m\binom{n-r}{m}(1-e^{-(\alpha y^{\beta})^2}[1+\theta(\alpha y^{\beta})^2])^{m+r-1}. \end{aligned}$$

Consequently, the density for the lowest and highest of $Y_{r:n}$, denoted as $k_{1:n}(y) = \min\{Y_1, Y_2, \ldots, Y_n\}$ and $k_{n:n}(t) = \max\{Y_1, Y_2, \ldots, Y_n\}$, are given, respectively, by

$$k_{1:n} = 2n\alpha^2 y^{2\beta-1} e^{-(\alpha y^\beta)^2}[1 - \theta + \theta(\alpha y^\beta)^2](e^{-(\alpha y^\beta)^2}[1 + \theta(\alpha y^\beta)^2])^{n-1} \tag{14}$$

and

$$k_{n:n} = 2n\alpha^2 y^{2\beta-1} e^{-(\alpha y^\beta)^2}[1 - \theta + \theta(\alpha y^\beta)^2](1 - e^{-(\alpha y^\beta)^2}[1 + \theta(\alpha y^\beta)^2])^{n-1}. \tag{15}$$

4 Entropy information

In this section, numerous information entropies are established. First, the Rényi entropy [29] ($R_1(\delta)$) is the measure of variation in uncertainty. The associated Rényi entropy of RT-BX model is

$$R_1(\delta) = \frac{1}{1-\delta}\log\left\{2^{\delta-1}\,\beta^{-1}\,\alpha^{2\delta+\beta(1+2\beta\delta-\delta)}\sum_{j=0}^{\infty}\binom{\delta}{j}\frac{\theta^j(1-\theta)^{\delta-j}}{\delta^{\frac{1+\delta(2\beta-1)}{2\beta}}}\Gamma\left(\frac{1+\delta(2\beta-1)}{2\beta}-1, 0\right)\right\}, \quad \delta \neq 1, \delta > 0. \tag{16}$$

Proof.

$$\begin{aligned} R_1(\delta) &= \frac{1}{1-\delta}\log\left(\int_0^\infty h_Y^\delta(y)\,\mathrm{d}y\right) \\ &= \frac{1}{1-\delta}\log\{2^\delta\alpha^{2\delta}y^{\delta(2\beta-1)}\,e^{-\delta(\alpha y^\beta)^2}(1-\theta+\theta(\alpha y^\beta)^2)^\delta\,\mathrm{d}y\}. \end{aligned}$$

Suppose that $t = (\alpha y^\beta)^2$, this implies $y = \left(\frac{t^{1/2}}{\alpha}\right)^{1/\beta}$ and $\mathrm{d}y = \frac{1}{2\beta\alpha^{1/\beta}}t^{\frac{1}{2\beta}-1}\mathrm{d}t$. The above equation can be reformulated as

$$R_1(\delta) = \frac{1}{1-\delta}\log\left\{\frac{2^{\delta-1}\alpha^{\beta(1+2\beta\delta-\delta)+2\delta}}{\beta}\sum_{j=0}^{\infty}\binom{\delta}{j}\theta^j(1-\theta)^{\delta-j}\int_0^\infty t^{\frac{1+\delta(2\beta-1)}{2\beta}-1}e^{-\delta t}\,\mathrm{d}t\right\}.$$

Now, take $w = \delta t$, which implies that $t = \frac{w}{\delta}$ and $\mathrm{d}t = \frac{\mathrm{d}w}{\delta}$. Thus,

$$\begin{aligned} R_1(\delta) &= \frac{1}{1-\delta}\log\left\{2^{\delta-1}\beta^{-1}\alpha^{2\delta+\beta(1+2\beta\delta-\delta)}\sum_{j=0}^{\infty}\binom{\delta}{j}\theta^j(1-\theta)^{\delta-j}\int_0^\infty\frac{w^{\frac{1+\delta(2\beta-1)}{2\beta}-1}}{\delta^{\frac{1+\delta(2\beta-1)}{2\beta}}}e^{-w}\,\mathrm{d}w\right\} \\ &= \frac{1}{1-\delta}\log\left\{2^{\delta-1}\beta^{-1}\alpha^{2\delta+\beta(1+2\beta\delta-\delta)}\sum_{j=0}^{\infty}\binom{\delta}{j}\frac{\theta^j(1-\theta)^{\delta-j}}{\delta^{\frac{1+\delta(2\beta-1)}{2\beta}}}\Gamma\left(\frac{1+\delta(2\beta-1)}{2\beta}-1, 0\right)\right\}, \end{aligned}$$

which completes the proof. □

Another uncertainty measure is the Shannon entropy [30] (R_2). It is expressed as

$$\begin{aligned} R_2 &= E[-\log(h_Y(y))] \\ &= -\log(2\alpha^2) - E[\log(e^{-(\alpha y^\beta)^2}y^{2\beta-1}(1-\theta+\theta(\alpha y^\beta)^2))] \\ &= -\log(2\alpha^2) + \alpha^2 E[y^{2\beta}] - E[\log(y^{2\beta-1})] - E[\log(1-\theta+\theta(\alpha y^\beta)^2)]. \end{aligned} \tag{17}$$

A new Havrda and Charvat entropy [31] ($R_3(\delta)$) of the RT-BX can be considered in this study. It can be formulated as

$$R_3(\delta) = \frac{2^{\delta-1}\alpha^{2\delta+\beta(1+2\beta\delta-\delta)}}{\beta(2^{1-\delta}-1)}\sum_{j=0}^{\infty}\binom{\delta}{j}\frac{\theta^j(1-\theta)^{\delta-j}}{\delta^{\frac{1+\delta(2\beta-1)}{2\beta}}}\Gamma\left(\frac{1+\delta(2\beta-1)}{2\beta}-1, 0\right) - 1, \quad \delta \neq 1, \delta > 0. \tag{18}$$

Now, the Tsallis entropy [32] $R_4(\delta)$ of the RT-BX distribution is defined by

$$R_4(\delta) = \frac{1}{\delta - 1}\left\{1 - \frac{2^{\delta-1}\alpha^{2\delta+\beta(1+2\beta\delta-\delta)}}{\beta}\sum_{j=0}^{\infty}\binom{\delta}{j}\frac{\theta^j(1-\theta)^{\delta-j}}{\delta^{\frac{1+\delta(2\beta-1)}{2\beta}}}\Gamma\left(\frac{1+\delta(2\beta-1)}{2\beta} - 1, 0\right) - 1\right\}, \quad \delta \neq 1, \delta > 0. \tag{19}$$

Finally, the Arimoto entropy [33] ($R_5(\delta)$) associated with the RT-BX model is represented by

$$R_5(\delta) = \frac{\delta}{\delta - 1}\left\{\frac{2^{\frac{1}{\delta}(\delta-1)}\alpha^{\frac{1}{\delta}(2\delta+\beta(1+2\beta\delta-\delta))}}{\beta^{\frac{1}{\delta}}}\left(\sum_{j=0}^{\infty}\binom{\delta}{j}\frac{\theta^j(1-\theta)^{\delta-j}}{\delta^{\frac{1+\delta(2\beta-1)}{2\beta}}}\Gamma\left(\frac{1+\delta(2\beta-1)}{2\beta} - 1, 0\right)\right)^{1/\delta} - 1\right\}. \tag{20}$$

The numerical vales of the suggested entropy information are displayed in Tables 3 and 4 based on numerous selected parameters θ, α, β, and δ and Figures 5 and 6 show the sketches of the 3D plots of this information entropy.

Table 3: Several entropy information records for $\delta = 0.75$ and $\theta = 0.5$

	α	$R_1(\delta)$	R_2	$R_3(\delta)$	$R_4(\delta)$	$R_5(\delta)$
$\beta = 0.5$	0.25	4.2854	4.1676	10.1439	7.6772	9.5168
	0.75	2.0881	1.9703	3.6228	2.7418	3.0174
	1	1.5128	1.3950	2.4293	1.8386	1.9673
	1.25	1.0665	0.9487	1.6149	1.2222	1.2807
$\alpha = 1$	0.25	2.1838	0.9487	3.8385	2.9051	3.2125
	0.75	1.0852	0.9487	1.6473	1.2467	1.3075
	1	0.7976	0.9487	1.1662	0.8826	0.9136
	1.25	0.5744	0.9487	0.8162	0.6177	0.6331
$\alpha = 1.5$	0.25	1.332	0.9487	2.0885	1.5806	1.6768
	0.75	0.5996	0.9487	0.8547	0.6469	0.6637
	1.25	0.4078	0.9487	0.5673	0.4293	0.4368
	1.75	0.2591	0.9487	0.3536	0.2676	0.2706

Table 4: Several entropy information records for $\delta = 1.5$ and $\theta = 0.75$

	α	$R_1(\delta)$	R_2	$R_3(\delta)$	$R_4(\delta)$	$R_5(\delta)$
$\beta = 0.5$	0.25	4.1699	4.2913	2.9898	1.7514	2.2527
	0.75	1.9727	2.0941	2.1409	1.2541	1.4457
	1	1.3973	1.5187	1.7165	1.0055	1.1170
	1.25	0.9510	1.0724	1.2921	0.7569	0.8150
$\alpha = 1$	0.25	2.0443	2.1254	2.1857	1.2804	1.4823
	0.75	0.9457	1.0268	1.2864	0.7536	0.8111
	1	0.6580	0.7392	0.9572	0.5607	0.5909
	1.25	0.4349	0.5160	0.6672	0.3908	0.4048
$\alpha = 1.5$	0.25	1.1403	1.2291	1.4837	0.8691	0.9486
	0.75	0.4079	0.4967	0.6300	0.3690	0.3814
	1	0.2161	0.3049	0.3497	0.2049	0.2085
	1.25	0.0674	0.1561	0.1131	0.0663	0.0666

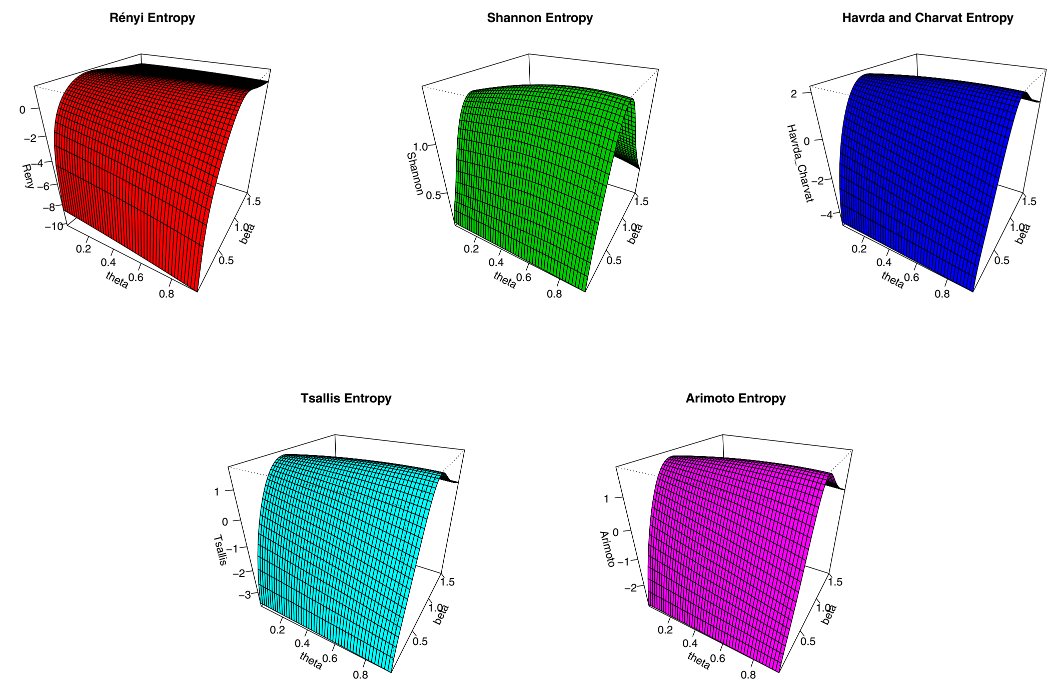

Figure 5: Plots for μ_1', Var, CV, $\mathcal{S}$, and $\mathcal{K}$ for $\alpha = 0.75$ and $\rho = 0.75$.

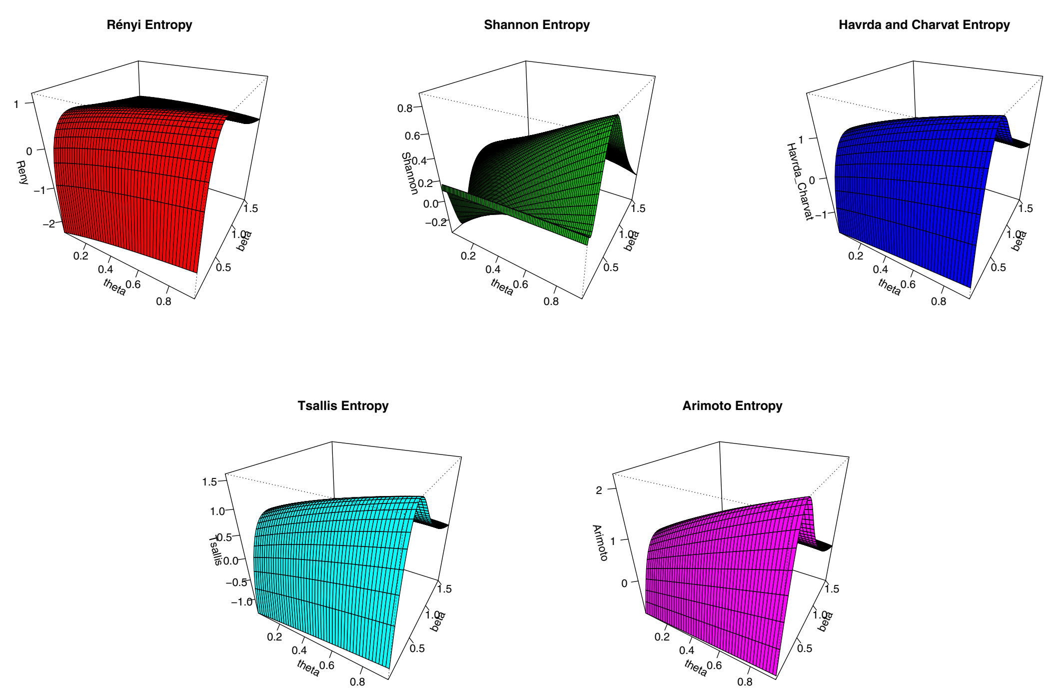

Figure 6: Plots for μ_1', Var, CV, $\mathcal{S}$, and $\mathcal{K}$ for $\alpha = 1.5$ and $\rho = 0.5$.

5 ML estimator

Let $\{y_1, y_2, \ldots, y_n\}$ be a random sample of the size n drawn from the RT-BX model. The associated likelihood function is now obtained as

$$\mathcal{L}(y, \vartheta) = \sum_{i=1}^{n} \log h_Y(y, \vartheta) - 2n\log(\alpha) + (2\beta - 1)\sum_{i=1}^{n} \log y_i - \alpha^2 \sum_{i=1}^{n} y_i^{2\beta} + \sum_{i=1}^{n} \log(1 - \theta + \theta(\alpha y_i^{\beta})^2). \tag{21}$$

On solving the below equations, we obtain the estimate of the given parameter of the RT-BX distribution under MLE method.

$$\frac{\partial \mathcal{L}(y,\vartheta)}{\partial \theta} = \sum_{i=1}^{n} \frac{(\alpha y_i^{\beta})^2 - 1}{1 - \theta + \theta(\alpha y_i^{\beta})^2}, \tag{22}$$

$$\frac{\partial \mathcal{L}(y,\vartheta)}{\partial \alpha} = \frac{2n}{\alpha} - 2\alpha \sum_{i=1}^{n} y_i^{2\beta} + 2\alpha\theta \sum_{i=1}^{n} \frac{y_i^{2\beta}}{1 - \theta + \theta(\alpha y_i^{\beta})^2},$$

and

$$\frac{\partial \mathcal{L}(y,\vartheta)}{\partial \beta} = 2\sum_{i=1}^{n} \log y_i - 2\alpha^2\theta \sum_{i=1}^{n} y_i^{2\beta} \log y_i + 2\sum_{i=1}^{n} \frac{y_i^{2\beta} \log y_i}{1 - \theta + \theta(\alpha y_i^{\beta})^2}. \tag{23}$$

The solution cannot be found analytically and must be obtained using numerical methods. Here in this study, the Newton-Raphson method is commonly applied to obtain the final estimate of the unknown parameters for the RT-BX model numerically.

6 Simulation analysis

In this section, Monte Carlo (MC) simulation studies are conducted to assess the performance of the recommended ML estimator tool for the newly generated RT-BX model by applying numerous sample sizes $n = \{300, 500, 700, 900, 1{,}000\}$ and various parameter set values of (θ, α, β) including Set 1 = (0.4, 2.25, 1.75), Set 2 = (0.5, 2.5, 2), Set 3 = (0.6, 2.75, 2.25), and Set 4 = (0.75, 3, 2.5). By using equation (10), we can generate a random sample of the RT-BX model. The computations were obtained employing the R program with a function **optim** for Newton-Raphson technique by taking the values of α, β, and θ as Set 1, Set 2, Set 3, and Set 4, respectively. The following algorithm describes the steps of random generating process from the suggested model:

(1) Obtain q from the uniform distribution $\mathcal{U}[0,1]$.
(2) In the same way, obtain y with the formula

$$y = \left\{\alpha^{-1}\left[-\frac{1}{\theta} - W_{-1}\left(\frac{u-1}{\theta e^{\frac{1}{\theta}}}\right)\right]^{1/2}\right\}^{1/\beta}.$$

Table 5: Numerical values of the RT-BX model simulation for Set 1

Sample size	**Est.**	$\hat{\theta}$	$\hat{\alpha}$	$\hat{\beta}$
300	AE	0.3776	2.2036	1.7313
	AB	0.0224	0.0464	0.0187
	MSE	0.0748	0.0250	0.0285
500	AE	0.3702	2.2066	1.7441
	AB	0.0218	0.0434	0.0059
	MSE	0.0650	0.0232	0.0219
700	AE	0.3785	2.2114	1.7469
	AB	0.0215	0.0386	0.0031
	MSE	0.0580	0.0185	0.0215
900	AE	0.3859	2.2131	1.7386
	AB	0.0141	0.0369	0.0014
	MSE	0.0522	0.0164	0.0165
1,000	AE	0.3941	2.2229	1.7568
	AB	0.0059	0.0271	0.0013
	MSE	0.0461	0.0123	0.0150

Table 6: Numerical values of the RT-BX model simulation for Set 2

Sample size	Est.	$\hat{\theta}$	$\hat{\alpha}$	$\hat{\beta}$
300	AE	0.4210	2.1441	1.7185
	AB	0.0790	0.3559	0.2815
	MSE	0.0916	0.0909	0.1528
500	AE	0.4374	2.4401	2.0159
	AB	0.0626	0.0599	0.0359
	MSE	0.0638	0.0236	0.0926
700	AE	0.4775	2.4701	1.9983
	AB	0.0225	0.0299	0.0217
	MSE	0.0559	0.0167	0.0310
900	AE	0.4816	2.4620	1.9836
	AB	0.0184	0.0280	0.0164
	MSE	0.0460	0.0118	0.0268
1,000	AE	0.4836	2.4666	1.9955
	AB	0.0174	0.0234	0.0045
	MSE	0.0373	0.0115	0.0180

Table 7: Numerical values of the RT-BX model simulation for Set 3

Sample size	Est.	$\hat{\theta}$	$\hat{\alpha}$	$\hat{\beta}$
300	AE	0.5693	2.6216	2.1687
	AB	0.0307	0.1284	0.0813
	MSE	0.0747	0.2479	0.2110
500	AE	0.5710	2.722	2.2628
	AB	0.0290	0.0480	0.0428
	MSE	0.0553	0.1148	0.0827
700	AE	0.5759	2.7183	2.2553
	AB	0.0241	0.0317	0.0383
	MSE	0.0460	0.0377	0.0465
900	AE	0.5845	2.7238	2.2706
	AB	0.0155	0.0262	0.0206
	MSE	0.0397	0.0111	0.0347
1,000	AE	0.5925	2.7224	2.2585
	AB	0.0150	0.0226	0.0085
	MSE	0.0304	0.0077	0.0276

After repeating the generating process $M = 1{,}000$ times, we compute the indicators mean estimate (AE), mean biases (AB), and average mean square errors (MSEs) which can be defined by

$$\mathrm{AE} = \frac{1}{M}\sum_{i=1}^{M}\hat{\varrho}, \quad \mathrm{AB} = \frac{1}{M}\sum_{i=1}^{M}|\hat{\varrho} - \varrho|, \quad \mathrm{MSE} = \frac{1}{M}\sum_{i=1}^{M}(\hat{\varrho} - \varrho)^2,$$

where $\varrho = (\theta, \alpha, \beta)$.

The results of these simulation experiments are reported in Tables 5–8. Based on the findings presented in Tables 5–8, we can conclude that the final estimates are generally constant and tend to the initial parameters. Also, for all parameter sets, if we increase n, the ABs and MSEs decrease, which ensures that the suggested ML estimators are consistent and asymptotically unbiased, where (Est) is the estimated values.

Table 8: Numerical values of the RT-BX model simulation for Set 4

Sample size	Est.	$\hat{\theta}$	$\hat{\alpha}$	$\hat{\beta}$
300	AE	0.7052	2.9877	2.5768
	AB	0.0448	0.0923	0.0768
	MSE	0.0473	0.0808	0.0952
500	AE	0.7365	2.9586	2.5387
	AB	0.0135	0.04140	0.0387
	MSE	0.0464	0.0659	0.0687
700	AE	0.7405	2.9863	2.5316
	AB	0.0095	0.01370	0.0316
	MSE	0.0405	0.0148	0.0557
900	AE	0.7481	2.9901	2.5224
	AB	0.0079	0.0099	0.0224
	MSE	0.0375	0.0088	0.0484
1,000	AE	0.7494	2.9982	2.5686
	AB	0.0306	0.0018	0.0186
	MSE	0.00578	0.0066	0.0446

7 Data analysis

Here we applied three real-life data sets to see the applicability, flexibility, and potentiality of the proposed RT-BX distribution. We apply the same data sets to compare the suggested model with the BX, transmuted log normal (T-LN), transmuted Weibul (T-Wei), transmuted log logistic (T-LL), and Extended exponential (Ex-Exp) distributions. Most of those models have received great attention in modeling several fields of data sets. It is often useful and necessary to check whether the considered model fit the data properly or not, and therefore, we use different standard metrics including the estimation of parameters, Kolmogorov-Smirnov ($\mathcal{KS}$) distance with its associate p-value ($\mathcal{PV}$), Akaike Information criterion ($\mathcal{A}_1$), and Bayesian Information criterion ($\mathcal{B}_1$). These results are reported in Table 9. From these results and based on the p-value, obviously, the numerical values of Table 9 demonstrate that the RT-BX model has a better fit to fit the three data sets. The plots of the pdfs (besides the data

Table 9: Distribution performance and information criterion values based on given three data sets

Data	Distribution	$\hat{\theta}$	$\hat{\alpha}$	$\hat{\beta}$	$\mathcal{KS}$	$\mathcal{PV}$	$\mathcal{A}_1$	$\mathcal{B}_1$
	RT-BX	0.5551	0.2993	1.1546	0.1078	0.7402	141.668	146.734
	BX		0.2090	1.2555	0.1281	0.5272	143.363	146.741
	T-LN	−0.6240	0.7873	0.6498	0.1656	0.2225	156.596	161.663
1	T-Wei	−0.3758	2.3622	3.222	0.1108	0.7095	142.411	147.478
	T-LL	−0.2486	3.0599	0.3598	0.1661	0.2197	157.563	162.630
	Ex-Exp		0.6228	3.5734	0.1657	0.2216	156.853	161.23
	RT-BX	0.7044	0.4257	2.3571	0.1412	0.1620	34.552	40.981
	BX		0.2745	2.6809	0.1744	0.0432	38.960	42.247
	T-LN	−0.638	0.2983	0.2610	0.2075	0.0087	56.300	62.729
1	T-Wei	−0.6069	4.7418	1.5204	0.1522	0.1078	35.070	41.50
	T-LL	−0.5583	6.0109	0.7142	0.1745	0.0430	39.030	42.559
	Ex-Exp		2.6118	31.357	0.2290	0.0026	66.767	71.053
	RT-BX	0.4467	0.4387	0.5598	0.0839	0.7244	377.838	384.496
	BX		0.3260	0.6124	0.0886	0.6593	377.934	384.779
	T-LN	−0.5682	1.0099	1.1304	0.1421	0.1278	391.477	398.136
3	T-Wei	−0.4189	1.0684	4.9840	0.0912	0.6225	378.221	384.880
	T-LL	−0.1735	1.6762	0.2538	0.0983	0.5260	381.345	387.004
	Ex-Exp		0.2020	1.3144	0.1079	0.4064	387.669	392.108

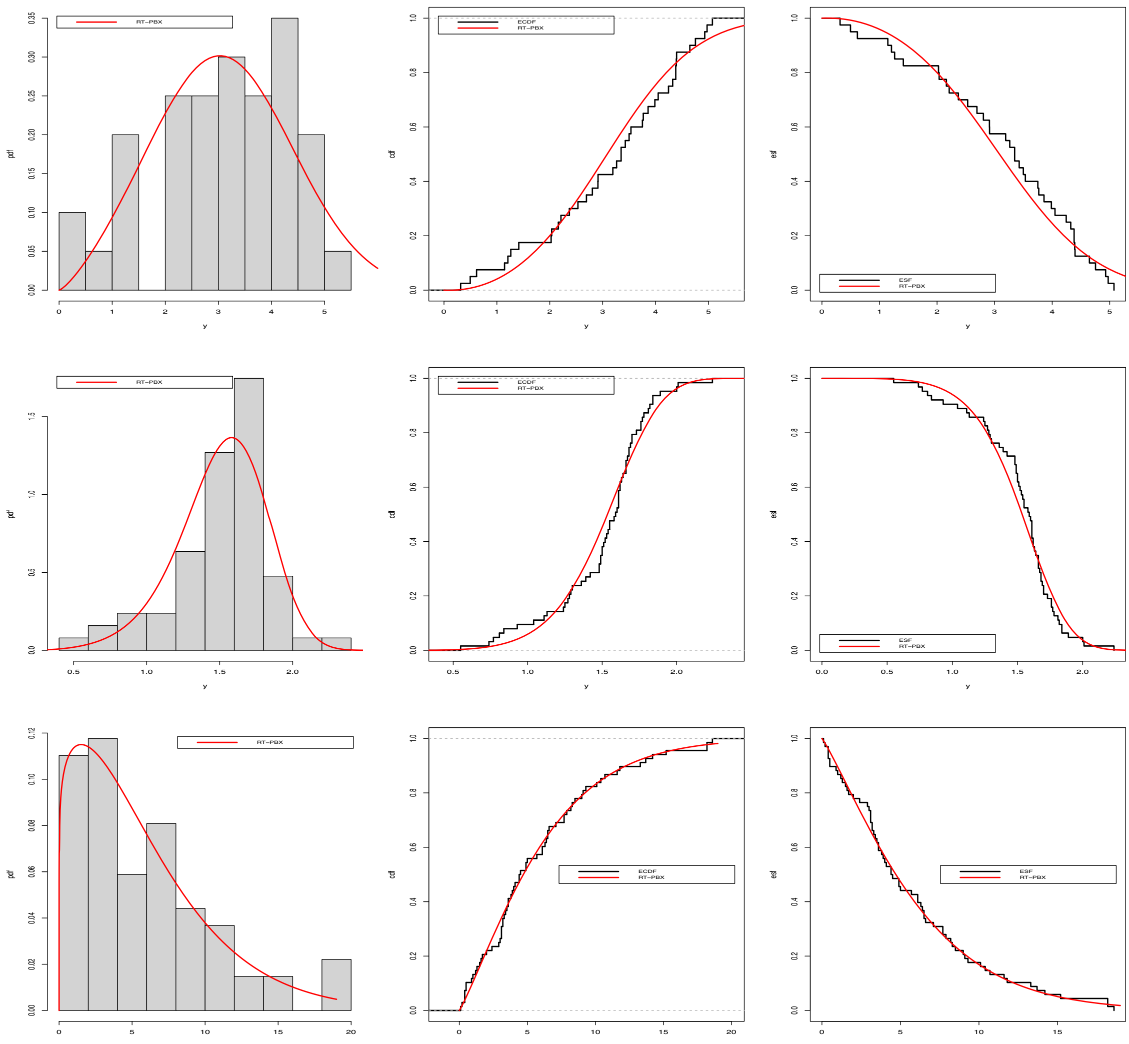

Figure 7: Estimated density, cumulative distribution, and survival function of the RT-BX model by applying the three considered data sets.

histogram), cdfs, and survival functions in Figure 7 ensure this conclusion. Further, Figures 8–10 draw the estimated density and cumulative distribution of all fitted models, and we can conclude from these figures that the recommended RT-BX model is more adequate for analyzing the three data sets.

7.1 First data set

The first data set was reported by Alshawarbeh et al. [34] and it represents 40 leukemia patients drawn from Saudi Arabia health ministry hospital. The values of the proposed data set are shown in Table 10.

7.2 Second data set

Here this data set contains 63 values and considered the strengths of 1.5 cm glass fibers. The suggested data set is applied by Smith and Naylor [35] and it is summarized in Table 11.

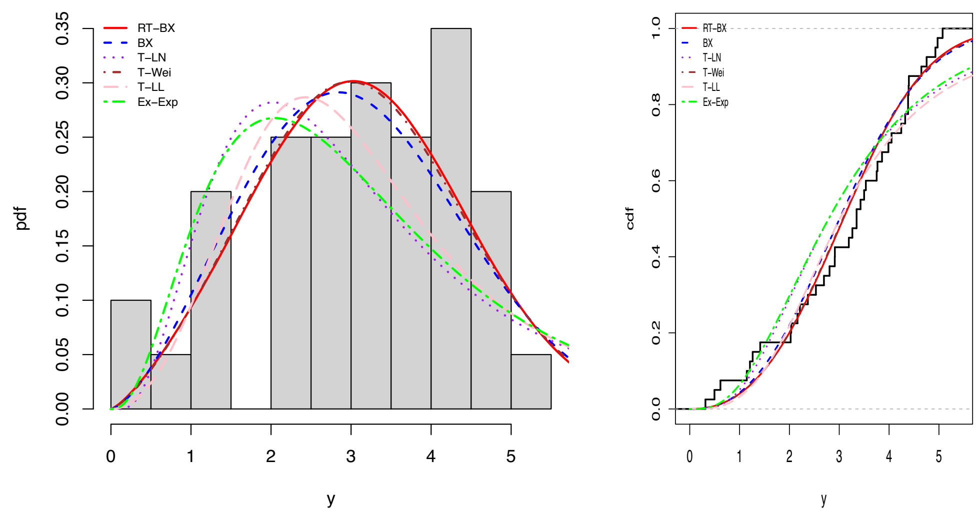

Figure 8: Estimated density, cdf plots for fitting proposed models using first data set.

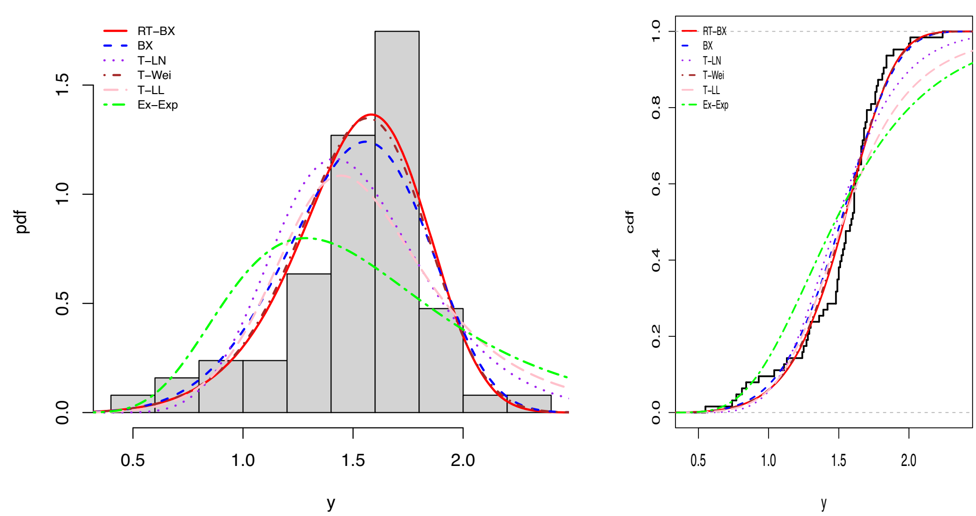

Figure 9: Estimated density, cdf plots for fitting proposed models using second data set.

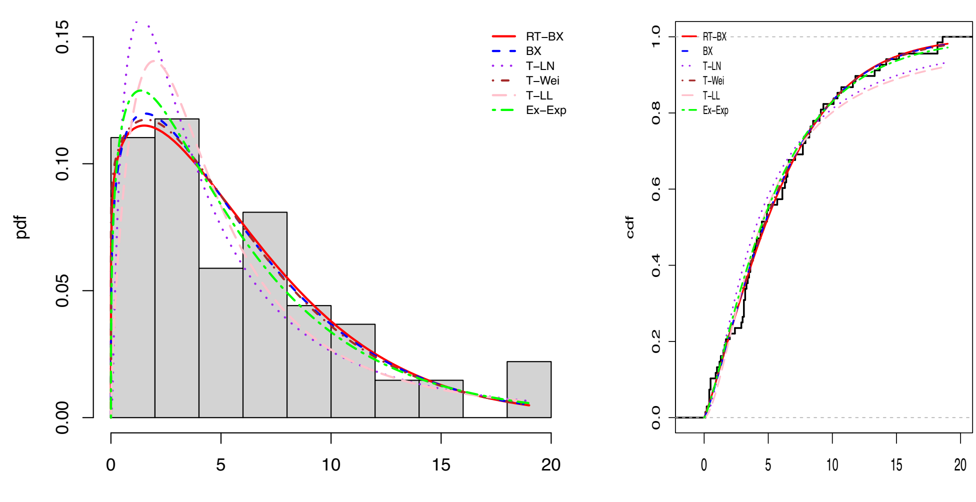

Figure 10: Estimated density, cdf plots for fitting proposed models using third data set.

Table 10: Values of data set 1

0.315	0.496	0.616	1.145	1.208	1.263	1.414	2.025	2.036	2.162
2.211	2.370	2.532	2.693	2.805	2.910	2.912	3.192	3.263	3.348
3.348	3.427	3.499	3.534	3.767	3.751	3.858	3.986	4.049	4.244
4.323	4.381	4.392	4.397	4.647	4.753	4.929	4.973	5.074	4.381

Table 11: Values of the strengths of 1.5 cm glass fibers

0.55	0.93	1.25	1.36	1.49	1.52	1.58	1.61	1.64	1.68
1.73	1.81	2	0.74	1.04	1.27	1.53	1.59	1.61	1.66
1.68	1.76	1.82	2.01	0.77	1.11	1.28	1.42	1.5	1.54
1.6	1.62	1.76	1.84	2.24	0.81	1.13	1.29	1.48	1.5
1.55	1.61	1.62	1.66	1.7	1.77	1.84	0.84	1.48	1.51
1.55	1.61	1.63	1.67	1.7	1.78	1.89	1.39	1.49	1.66
1.69	1.24	1.3							

7.3 Third data set

The source of this data is taken from Patil and Rao [36] as well as Almetwally and Meraou provide it [37]. The proposed data set represents the locations of the 68 stakes found while walking $F = 1{,}000$ m and looking $l = 20$ m on either side of the transect line. The records of data set are given in Table 12.

Table 13 shows the numerous basic statistics of the observed data sets, and Figure 11 displays the numerous non-parametric plots notably the scaled total time on the test (TTT), the probability-probability (PP), and box plots.

Table 12: Sixty eight stakes found while walking and looking data set

2.0	0.5	10.4	3.6	0.9	1.0	3.4	2.9	8.2	6.5	5.7	3.0	4.0
0.1	11.8	14.2	2.4	1.6	13.3	6.5	8.3	4.9	1.5	18.6	0.4	0.4
0.2	11.6	3.2	7.1	10.7	3.9	6.1	6.4	3.8	15.2	3.5	3.1	7.9
18.2	10.1	4.4	1.3	13.7	6.3	3.6	9.0	7.7	4.9	9.1	3.3	8.5
6.1	0.4	9.3	0.5	1.2	1.7	4.5	3.1	3.1	6.6	4.4	5.0	3.2
7.7	18.2	4.1										

Table 13: Basic mathematical measures for the three suggested data

Data	Min	Q_1	Q_2	μ'	Q_3	Max	$\mathcal{S}$	$\mathcal{K}$
1	0.315	2.199	3.348	3.116	4.264	5.074	0.477	0.834
2	0.550	1.375	1.590	1.507	1.685	2.240	0.878	0.8001
3	0.100	2.975	4.450	5.853	8.225	18.600	1.020	0.470

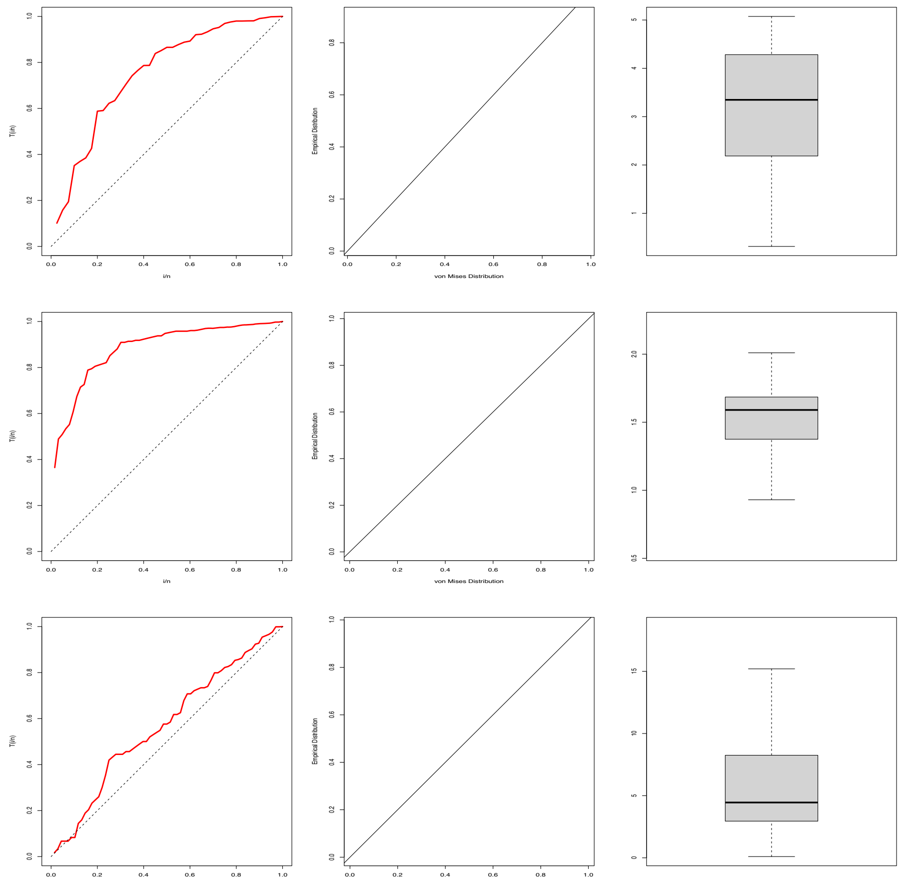

Figure 11: TTT, PP, and box plots for the selected data sets.

8 Conclusion

A novel approach to BXD is defined in this work using a record-based transmuted tool, which is a powerful tool in modeling numerous types of data sets, notably skewed, complex, asymmetric, and symmetric. The recommended model has three parameters, and its density has different shapes. Further, we provide the maximum likelihood approach for estimating the model parameters, as well as several simulation experiments are performed to demonstrate the efficiency of the suggested estimation technique. At the end, the applicability of the proposed distribution is demonstrated using three real data sets. The obtained results illustrate that our recommended model is the best fitting distribution for fitting the three recommended data sets.

Funding information: The author states no funding involved.

Author contributions: The author confirms the sole responsibility for the conception of the study, presented results, and manuscript preparation.

Conflict of interest: The author states no conflicts of interest.

Data availability statement: All data sets used in this study are contained in this article.

References

[1] G. Hamedani, M. Korkmaz, N. Butt, and H. Yousof, *The type II quasi Lambert family: properties, characterizations and different estimation methods*, Pak. J. Stat. Oper. Res. **18** (2022), no. 4, 963–983, DOI: https://doi.org/10.18187/pjsor.v18i4.3907.

[2] M. Cordeiro and R. Brito, *The beta power distribution*, Braz. J. Probab. Stat. **26** (2012), no. 1, 88–112, DOI: http://dx.doi.org/10.1214/10-BJPS124.

[3] A. Marshall and I. Olkin, *A new method for adding a parameter to a family of distributions with application to the exponential and Weibull families*, Biometrika **84** (1997), no. 3, 641–652, DOI: https://doi.org/10.1093/biomet/84.3.641.

[4] A. Mahdavi and D. Kundu, *A new method for generating distributions with an application to exponential distribution*, Comm. Statist. Theory Methods **46** (2017), no. 13, 6543–6557, DOI: https://doi.org/10.1080/03610926.2015.1130839.

[5] A. Hassan, R. Mohamd, M. Elgarhy, and A. Fayomi, *Alpha power transformed extended exponential distribution: properties and applications*, J. Nonlinear Sci. Appl. **12** (2018), no. 4, 62–67, DOI: http://dx.doi.org/10.22436/jnsa.012.04.05.

[6] T. Moakofi, B. Oluyede, and F. Chipepa, *Type II exponentiated half-logistic Topp-Leone Marshall-Olkin-G family of distributions with applications*, Heliyon **7** (2021), no. 12, e08590.

[7] J. Eghwerido, S, Zelibe, and E. Efe-Eyefia, *Gompertz-alpha power inverted exponential distribution: properties and applications*, Thail. Stat. **18** (2020), no. 3, 319–332, https://ph02.tci-thaijo.org/index.php/thaistat/article/view/241282.

[8] L. Sapkota, V. Kumar, A. Gemeay, M. Bakr, O. Balogun, and A. Muse, *New Lomax-G family of distributions: Statistical properties and applications*, AIP Adv. **13** (2023), no. 9, 095128, DOI: https://doi.org/10.1063/5.0171949.

[9] M. Meraou and M. Raqab, *Statistical properties and different estimation procedures of Poisson Lindley distribution*, J. Stat. Theory Appl. **20** (2021), no. 1, 33–45, DOI: https://doi.org/10.2991/jsta.d.210105.001.

[10] M. Meraou, N. Al-Kandari, M. Raqab, and D. Kundu, *Analysis of skewed data by using compound Poisson exponential distribution with applications to insurance claims*, J. Stat. Comput. Simul. **92** (2021), no. 5, 928–956, DOI: https://doi.org/10.1080/00949655.2021.1981324.

[11] B. Thomas and V. Chacko, *Power generalized DUS transformation in Weibull and Lomax distributions*, Reliability: Theory & Applications **1** (2023), no. 72, 368–384.

[12] N. Balakrishnan and M. He, *A record-based transmuted family of distributions*, in: I. Ghosh, N. Balakrishnan, H. K. T. Ng (Eds.), Advances in Statistics Theory and Applications, Emerging Topics in Statistics and Biostatistics, Springer, Cham, Switzerland, 2021, pp. 3–24, DOI: https://doi.org/10.1007/978-3-030-62900-7_1.

[13] C. Tanis and B. Saracoglu, *On the record-based transmuted model of Balakrishnan and He based on Weibull distribution*, Comm. Statist. Simulation Comput. **51** (2022), no. 8, 4204–4224, DOI: https://doi.org/10.1080/03610918.2020.1740261.

[14] M. Arshad, M. Khetan, V. Kumar, and A. Pathak, *Record-based transmuted generalized linear exponential distribution with increasing, decreasing and bathtub shaped failure rates*, Comm. Statist. Simulation Comput. **53** (2022), no. 7, 1–25, DOI: https://doi.org/10.1080/03610918.2022.2106494.

[15] C. Tanis, *A new Lindley distribution: applications to COVID-19 patients data*, Soft Comput. **28** (2024), 2863–2874, DOI: https://doi.org/10.1007/s00500-023-09339-7.

[16] K. Sakthivel and V. Nandhini, *Record-based transmuted power Lomax distribution: properties and its applications in reliability*, Reliability: Theory & Applications **17** (2022), no. 4, 574–592.

[17] A. L. Sobhi and M. Mashail, *Moments of dual generalized order statistics and characterization for transmuted exponential model*, Comput. J. Math. Stat. Sci. **1** (2022), no. 1, 42–50.

[18] R. A. Mohamed, I. Elbatal, E. M. ALmetwally, M. Elgarhy, and H. M. Almongy, *Bayesian estimation of a transmuted Topp-Leone length biased exponential model based on competing risk with the application of electrical appliances*, Mathematics **10** (2022), no. 21, 4042.

[19] V. Kumar, A. Chakraborty, M. Arshad, and A. Tiwari, *A new Nadarajah-Haghighi distribution with applications*, Res. Square **1** (2024), DOI: https://doi.org/10.21203/rs.3.rs-3825940/v1.

[20] R. Usman and M. Ilyas, *The power Burr Type X distribution: properties, regression modeling and applications*, Punjab Univ. J. Math. **52** (2020), 27–44.

[21] A. A. Al-Babtain, I. Elbatal, H. Al-Mofleh, A. M. Gemeay, A. Z. Afify, and A. M. Sarg, *The flexible Burr XG family: properties, inference, and applications in engineering science*, Symmetry **13** (2021), no. 3, 474.

[22] A. Fayomi, A. Hassan, H. Baaqeel, and E. Almetwally, *Bayesian inference and data analysis of the unit-power Burr X distribution*, Axioms **2023** (2023), no. 12, 297, DOI: https://doi.org/10.3390/axioms12030297.

[23] M. Raqab and D. Kundu, *Burr type X distribution: revisited*, J. Probab. Stat. Sci. **4** (2006), 179–193.

[24] E. Yıldırım, E. Ilıkkan, A. Gemeay, N. Makumi, M. Bakr, and O. Balogun, *Power unit Burr-XII distribution: Statistical inference with applications*, AIP Adv. **13** (2023), no. 10, 105107.

[25] M. Korkmaz, E. Altun, H. Yousof, A. Afify, and S. Nadarajah, *The Burr X Pareto distribution: properties, applications and VaR estimation*, J. Risk Financial Manag. **11** (2018), no. 1, 1–16, DOI: https://doi.org/10.3390/jrfm11010001.

[26] F. Merovci, M. Khaleel, and N. Ibrahim, *The beta Burr type X distribution properties with application*, SpringerPlus **5** (2016), no. 697, 1–18, DOI: https://doi.org/10.1186/s40064-016-2271-9.

[27] J. G. Surles and W. J. Padgett, *Some properties of a scaled Burr type X distribution*, Inference **128** (2005), no. 1, 271–280, DOI: https://doi.org/10.1016/j.jspi.2003.10.003.

[28] R. Glaser, *Bathtub and related failure rate characterizations*, J. Amer. Statist. Assoc. **75** (1980), no. 371, 667–672, DOI: https://doi.org/10.1080/01621459.1980.10477530.

[29] A. Rényi, On measures of entropy and information, in: Proceedings 4th Berkeley Symposium on Mathematical Statistics and Probability, University of California Press, 1960.

[30] C. Shannon, *A mathematical theory of communication*, Bell Syst. Tech. J. **27** (1948), 379–423, DOI: https://doi.org/10.1002/j.1538-7305.1948.tb01338.x.

[31] J. Havrda and F. Charvat, *Quantification method of classification processes: concept of structural-entropy*, Kybernetika **3** (1967), no. 1, 30–35, DOI: http://eudml.org/doc/28681.

[32] C. Tsallis, *Possible generalization of Boltzmann-Gibbs statistics*, J. Stat. Phys. **52** (1988), no. 1–2, 479–487, DOI: https://doi.org/10.1007/BF01016429.

[33] S. Arimoto, *Information-theoretical considerations on estimation problems*, Inf. Control **19** (1971), no. 3, 181–194, DOI: https://doi.org/10.1016/S0019-9958(71)90065-9.

[34] E. Alshawarbeh, M. Z. Arshad, M. Z. Iqbal, M. Ghamkhar, A. Al Mutairi, M. A. Meraou, et al., *Modeling medical and engineering data using a new power function distribution: theory and inference*, J. Radiat. Res. Appl. Sci. **17** (2024), no. 1, 1–15, DOI: https://doi.org/10.1016/j.jrras.2023.100787

[35] R. Smith and J. Naylor, *A comparison of maximum likelihood and Bayesian estimators for three-parameter Weibull distribution*, Appl. Stat. **36** (1987), 358–369, DOI: https://doi.org/10.2307/2347795.

[36] G. Patil and C. Rao, *Environmental Statistics*, Handbook of Statistics, vol. 12, Elsevier B.V., 1994.

[37] E. Almetwally and M. Meraou, *Application of environmental data with new extension of Nadarajah-Haghighi distribution*, Comput. J. Math. Stat. Sci. **1** (2022), no. 1, 26–41, DOI: https://doi.org/10.21608/cjmss.2022.271186.